UDC 539.4

In-Service Inspections of Thick Walled Concrete Structures

L. Pecinka[a] and S. Moravka[b]

[a] Nuclear Research Institute, Rez, Czech Republic

[b] New Technologies Research Centre, University of West Bohemia, Pilsen, Czech Republic

УДК 539.4

Технический контроль при эксплуатации толстостенных бетонных конструкций

Л. Печинка[а], С. Моравка[б]

[а] Институт ядерных исследований, Рез, Чехия

[б] Исследовательский центр новых технологий, Западно-Богемский университет, Пльзень, Чехия

Основными проблемами ядерной энергетики являются контроль процесса старения и возобновление операционных лицензий существующих атомных станций. В качестве наиболее приоритетного направления контроля процесса старения бетонных конструкций используются так называемые ISI-методы для железобетонных толстостенных конструкций с недоступными для осмотра участками. Обсуждается научно-исследовательская программа в этой области, а также некоторые результаты, используемые в квалификационном анализе ISI-методов.

Ключевые слова: управление процессом старения, бетонные конструкции, метод эхо-удара, волновой процесс, армированные стержни, пустоты, наклонные трещины, образцы для испытаний.

Introduction. Ageing management and renewal of the operating license of existing nuclear power plants (NPP) are at present the main problems of nuclear power industry. For the ageing management of concrete structures OECD-Nuclear Energy Agency, the Committee on the Safety of Nuclear Installations (CSNI), Principal Working Group "Integrity and Ageing," subgroup "Ageing of Concrete Structures" reviewed national and international activities in this area including the relevant activities of other international agencies. A proposal for a CSNI program of workshops was developed to address specific technical issues, which were subdivided by OECD-NEA task group into three levels of priority:

First Priority:

– loss of pre-stressing force of post-tensioned concrete structures;

– ISI techniques for reinforced concrete structures having thick sections and areas not directly accessible for inspections.

Second Priority:

– viability of development of a performance based database;

– response of degraded structures (including FEM techniques).

Third Priority:

– instrumentation and monitoring;

– repair methods;

– criteria for condition assessment.

Characteristics of safety related concrete structures (in particular thickness of sections, congested reinforcement and restricted access) limit the application of NDE techniques. Quantification of these limitations and developments of methods to overcome them is driving research programs in a number of OECD Member States. In this paper is described research program of Nuclear Research Institute (NRI) Rez and results obtained.

1. **NRI Research Program**. The program is entitled "In-Service Inspections of Thick Walled Concrete Structures." Time of duration is from 2004 to 2007, sponsoring organizations are Ministry of Industry and Trade of Czech Republic and Czech Energy Utilities. Three ISI techniques were selected: Impact-Echo ultrasound and high frequency radar or betatron 7 MeV. NRI is the leading organization, cooperating organizations are Technical University Brno, Faculty of Civil Engineering and University of West Bohemia in Pilsen, New Technologies Research Centre. Time schedule is as follows:

2004

Mathematical modeling of the Impact-Echo method. Three tasks were selected:

– detection of reinforcing base;

– detection of surface crack with variable depth;

– detection of the void.

2005

– mathematical modeling of crack oblique to surface;

– design and fabrication of testing pieces.

2006

– measurements on the testing pieces;

– tuning the developed mathematical models.

2007

– additional measurements;

– in-situ measurements;

– qualification of selected ISI techniques.

2. **Discussion of Results Obtained**.

2.1. ***Mathematical Modeling of Impact-Echo Method***.

2.1.1. *Numerical Model and Its Properties*. The finite element method is being used for numerical simulation of the impact-echo method. Selecting the mesh and time step size appropriately, we respect the waves with length $\lambda_{\min} = 60$ mm and more. The sand particles are the size of up to 4 mm and the aggregates up to 16 mm, the concrete is poured, and the stressing is relatively very small at the tests. For this reason, the concrete mixture as well as the reinforcing steel can be modeled as a homogenous, isotropic, and elastic material.

The computational systems COSMOS/M and MSC-MARC/MENTAT were tested. Recent experimental data were used as well. Since the results yielded by MARC were substantially closer to the experiment, we further use the system MSC-MARC/MENTAT.

8-Node isoparametric elements with edge length of 5 mm and time step $\Delta t = 1.2$ μs were used in the calculations considering reinforcing. The diameter of a reinforcing bar is 40 mm, i.e., 8 elements. Unfortunately, we could not use elements of varying size for this type of problem (different cut-off-frequencies, spurious wave reflections. The 16 millions elements would be needed if we wish to model a 1×2 m portion of a wall 1 m thick in this way. Neither is possible to homogenize the wall, as we need to localize individual bars.

Elements with edge size of 3 cm and time integration step $\Delta t = 7$ μs are considered in calculating the walls with cracks. The presence of reinforcing bar must not however be respected because the minimum wavelength is 6 cm here. The experience gained in the earlier calculations and confrontations of numerical simulations with known analytic solutions were employed in the selection of numerical calculation parameters.

The elements with edge size of 3 cm that we have applied are capable of transferring the waves with the frequency of up to 70 kHz approximately without amplitude attenuation in the extreme case when the wavelength corresponds to two elements lengths. This frequency is called cut-off-frequency and should correspond to the time integration step so as to make the frequency limits given by temporal and by spatial discretization similar. Otherwise the calculation parameters have been chosen inconveniently – for example, the result with fine spatial discretization gained at considerable costs can be degraded by too rough temporal discretization and vice versa. Suitable selection of the time integration method (here, Newmark implicit integration) combined with spatial discretization method (here, consistent mass matrix) is also of great importance because it is advisable to prevent superposing the side effects of either discretization and, conversely, to eliminate them partly.

A blow of the testing hammer initializes the excitation. We estimate the blow is a force of 5,000 N acting for 36 μs. Taking into account the dimensions of the body, we consider the excitation as spot excitation.

We have employed the numerical implicit time integration by the Newmark method with modified coefficients $\beta = 0.275625$ and $\gamma = 0.55$. Retaining the unconditional stability of the method, this modification introduces a moderate numerical attenuation, which suppresses especially the spurious influence of higher frequencies. This option has proved suited even in the preceding similar calculations.

In addition, we tried to employ the elements with one-point reduced integration in order to accelerate the computation. The results don't differ substantially so that the reduced integration is in principle applicable with this type of a problem.

Although 3D problems are the matter, we tried out the possibility of treating them as a 2D case, namely plane stress and plane strain problems as well. The 2D and 3D results however substantially differ so that we must insist on 3D models.

2.1.2. *Testing the Possibility of Localizing Reinforcing Bars*. As first, we deal with the response of a concrete section of a wall 190×200 mm, 70 mm thick [1]. Elements with edge size of 5 mm have been employed. A distance of the same 70 mm separates the positions of excitation and measurement on the surface and their join, parallel to the specimen edge, passes through the middle of its upper

surface. Making use of the symmetry, the problem can be reduced to a half-size model involving 10,640 elements. On the second case, the geometry of the other model is identical, only that its lower half is made from steel while the upper one, where the excitation occurs and the response is sampled, is from concrete (like Fig. 1 without showing the reinforcing bar). The goal is to find out, how the waves reflect on the concrete-steel dividing plane and how they pass through it back after reflecting from the specimen's bottom. In the third case, one reinforcing bar 40 mm in diameter (Fig. 1) is inserted in the same concrete sample in position parallel to the surface and in the depth of 50 mm.

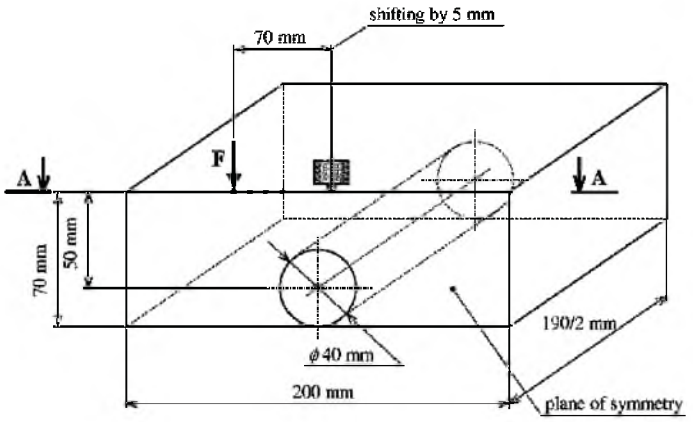

Fig. 1. Schema of reinforcing bar detection and localization testing.

Figures 2 and 3 show a comparison of time history of the displacements perpendicular to the surface in the three cases mentioned. The time point, at which the responses differ significantly, is near the share wavefront reflected from the concrete-steel dividing plane ($t = 39.02$ μs) or very accurately at the shear wavefront reflected on the inserted bar top ($t = 36.34$ μs). It can be therefore deduced that, in all probability, it is the very shear wave reflection, which brings the key information about the material-dividing plane to the surface and, as a result, it can be used for the reinforcing bars detection.

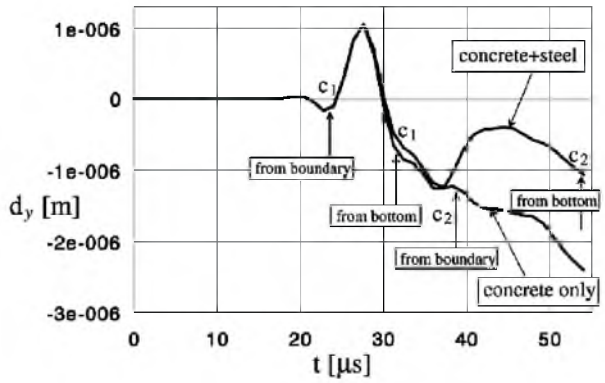

Fig. 2. Comparison of only concrete sample response with that of concrete-steel dividing plane sample.

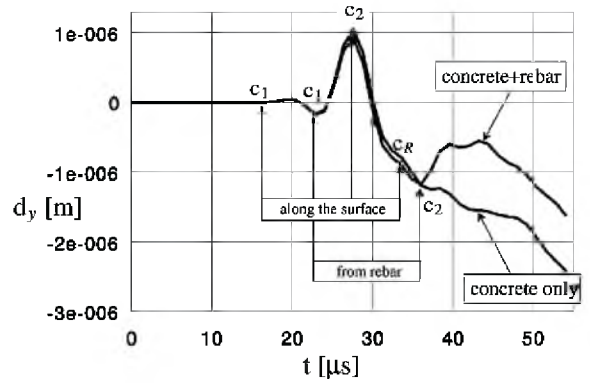

Fig. 3. Comparison of only concrete sample response with that of inserted reinforcing bar sample.

The testing of reinforcing bars numerical detection and localization will be further continued. It indeed will be impossible to model a solid wall (1 m thick), but we intend to enlarge considered area and to refine the discretization.

2.1.3. *Modeling Crack Detection and Localization*. We perform these simulations with a segment of a concrete wall having dimensions of 2 by 2 meters an 1 meter thick [1]. Owing to planar symmetry of the problem, it even now is possible to treat only one half of the body (Fig. 4). Elements with edge size of 3 cm (71,874 elements, 144 time steps with $\Delta t = 7$ μs) were used in the final calculation. It ends at the time of 1,001 μs, at which the results are about to commence to be degraded by the reflections from sample sidewalls. Step by step, the following problems are dealt with:

– Comparison calculation of thick plate response without any cracks to spot excitation by an experimental hammer at 67 points (excitation and measuring on the same surface).

– Response of a cracked thick plate to the spot excitation by a hammer at 68 wall surface points (one point extra is due the crack edge) (excitation, measuring, and crack on the same (accessible) surface).

– Response of a thick plate with crack on opposite (inaccessible) surface to the spot excitation at 67 wall surface points.

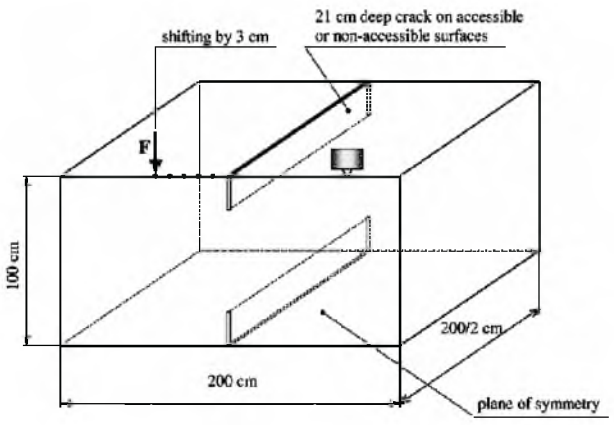

Fig. 4. Scheme of tasks for calculations of wall with surface cracks.

It is assumed that the crack has arisen due to tensile loading and that its surfaces are therefore not in the contact. An experiment would show whether this assumption is true.

Figure 5 presents a comparison of two time histories of displacement perpendicular to the surface. The excitation and measuring occurs on the same surface 20 cm apart. The first case is a flawless concrete wall while the other is a wall with a crack of 20 cm in depth midway between the exciting and measuring points. It is evidenced in the figure that the crack prevents the surface Rayleigh waves from passing through.

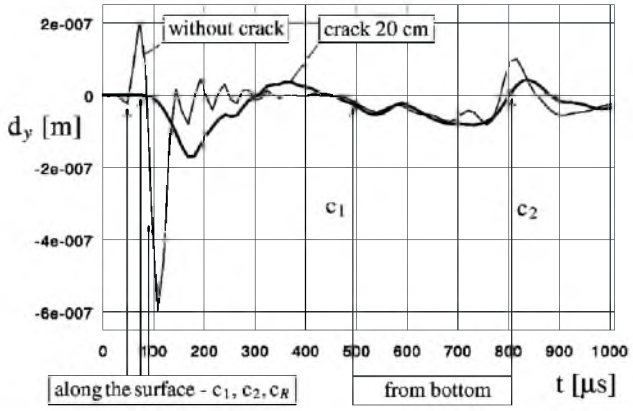

Fig. 5. Comparison of defectless sample response with sample with a crack of 20 cm in depth.

In case of a flawless wall, wall with a crack on accessible surface and wall with crack on inaccessible surface, we carry out a series of calculations for excitation advancing by 3 cm along a line two meters long and passing through the middle of the sample (Fig. 4). Thus 67 tasks are computed for each case of wall (or 68 since the crack produces an edge with another excited node). The runtime of one task is 25 resp. 23 hours on a 32-bit computer resp. 64-bit Itanium computer. The runtime are surprisingly small.

2.1.4. *Impact-Echo Method Modeling for the Detection and Localization of Cracks Variously Inclined to the Surface*. In this part of paper we numerically by FEM simulate propagation of elastic waves initiated by instrumental hammer impact in the surroundings of opened crack inclined to the surface at various angles [2]. The inclination of through-going straight 21 cm depth crack changes by 10 degrees, from 0 to 180°. Excitation place is shifting by 6 cm along the surface straight line perpendicular to the crack, while the time responses are recorded over all this line, i.e., before and behind of crack as well. For the task configuration see on Fig. 6.

(Convention: the crack inclination is measured from crack to surface by the direction toward the excitation place.)

It is possible to summarize the most essentials phenomena into some next notes:

1 – wave reflection:

The wave reflections from the crack very inclined to the surface are considerably different according to crack inclination direction, e.g., inclinations

40 and 140°, although the perpendicular depth of both these crack is the same. The Rayleigh surface wave and S-wave (i.e., second, shear, transversal) reflection from acute angles are considerably more significant than reflection from obtuse angles, when waves travel from opposite side of the crack. The example of time dependent responses is on Fig. 7.

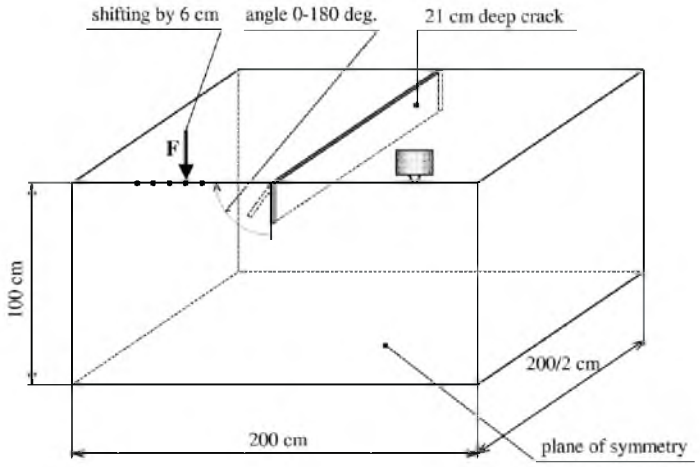

Fig. 6. The configuration of inclined cracks measuring.

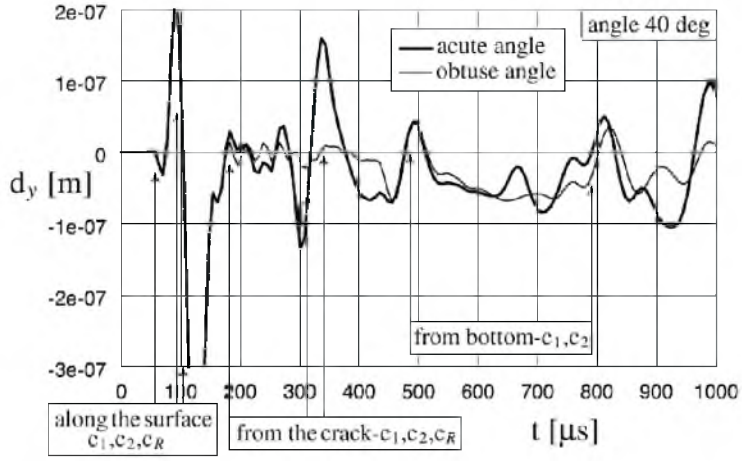

Fig. 7. The wave reflection from acute crack 40° inclined and from abuse crack 140° inclined. Time dependences of displacement perpendicular to the surface.

The greatest displacement due to Rayleigh surface wave reflection can be found for the crack inclination angle around 45°, not for 90°, as could be expected. Deformation energy more hardly passes through the acute angle "trap." See e.g., screen captures on Figs. 8 and 9.

The reflection from obtuse crack side, i.e., from angles approx. from 135° above, is very low. Wave motion as would be "slipping" inside of the body over the obtuse crack face. It can be demonstrated by Fig. 7 meant above and by screen capture on the Fig. 8 as well.

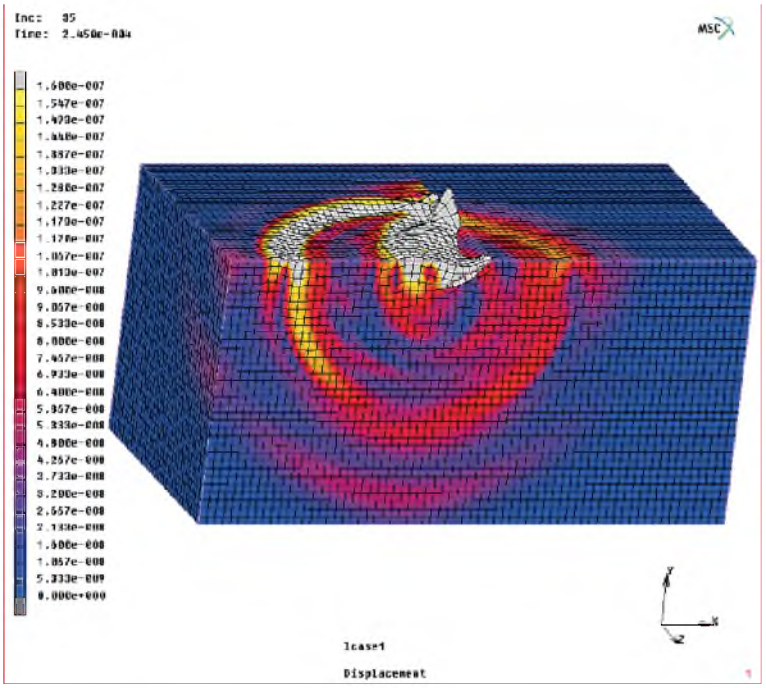

Fig. 8. The displacements in time 254 μs if the excitation is situated on the acute angle side.

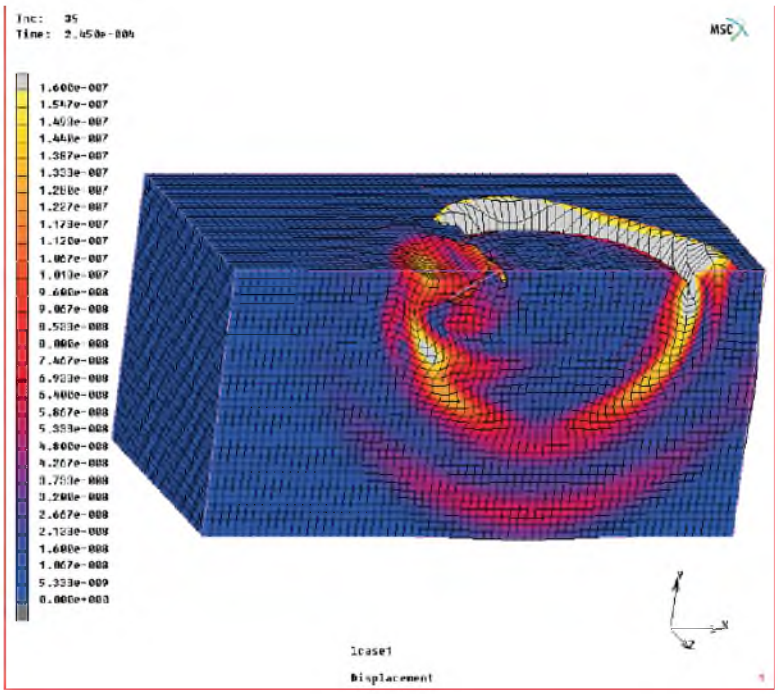

Fig. 9. The displacements in time 254 μs if the excitation is situated on the abuse angle side.

The waves shapes reflected from relatively acute angles (approx. up to 45°) considerably vary, like oscillate. So, to determine the inclination of such cracks according to the wave reflection shape would be very troublesome.

Currently (i.e., upon the acute angles) the arrival time of wave reflections is decreasing. As the acute crack inclines to the surface, the reflection approximately from the crack's root starts to build, in addition to the expected Rayleigh surface wave reflection from the crack mouth (Fig. 10a and 10b). Upon the obtuse angles (very inclined to the surface as well, but contrary) we can see reversed phenomenon, i.e., the delayed wave reflection from crack's root appears (Fig. 11a and 11b).

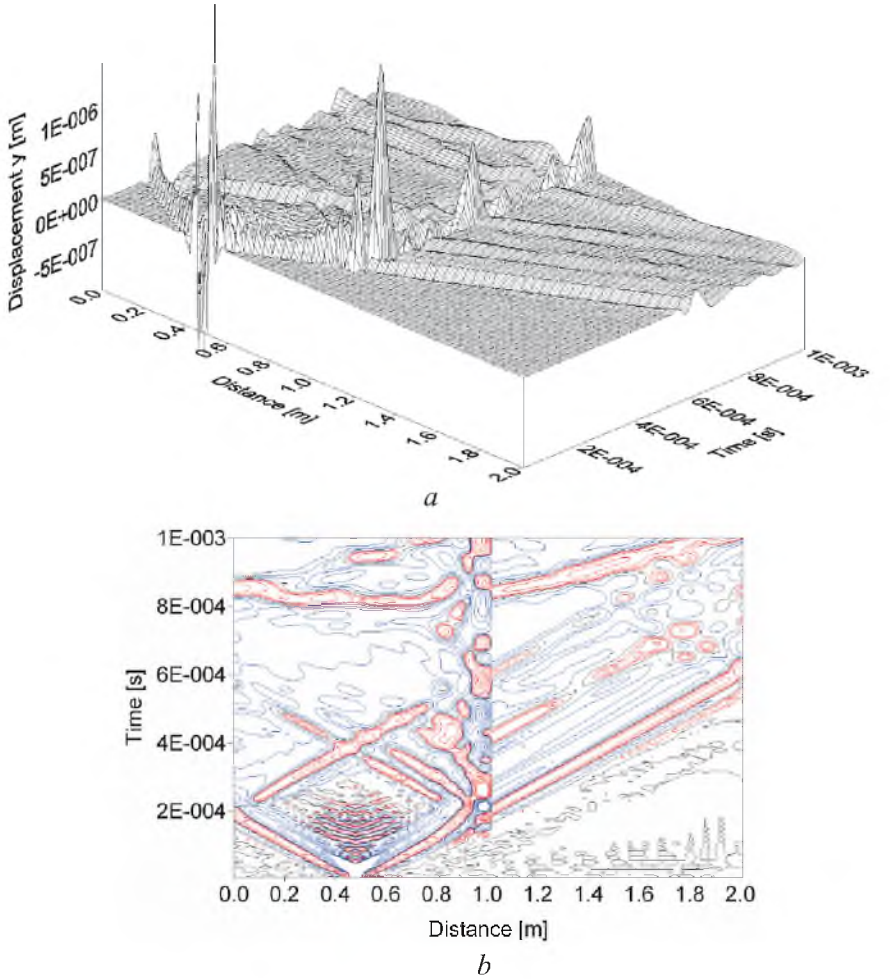

Fig. 10. Time responses from excitation in front of acute inclined crack (10°) at the nodes along whole surface line right-angle crossing the crack (*a*) and plan view (*b*).

2 – wave passing:

Wave motion passed through the very inclined cracks to the surface is greatly more damped down by the obtuse cracks (140° and above – Fig. 11a), than by acute cracks (approx. up to 40° – Fig. 10a). Once again (similar to reflections) R-wave as would be "slipping" inside of the body over the crack back and can develop enough up to sensor place. The waves passed through such contrary inclined cracks are more similar until at the relatively large distance from the crack.

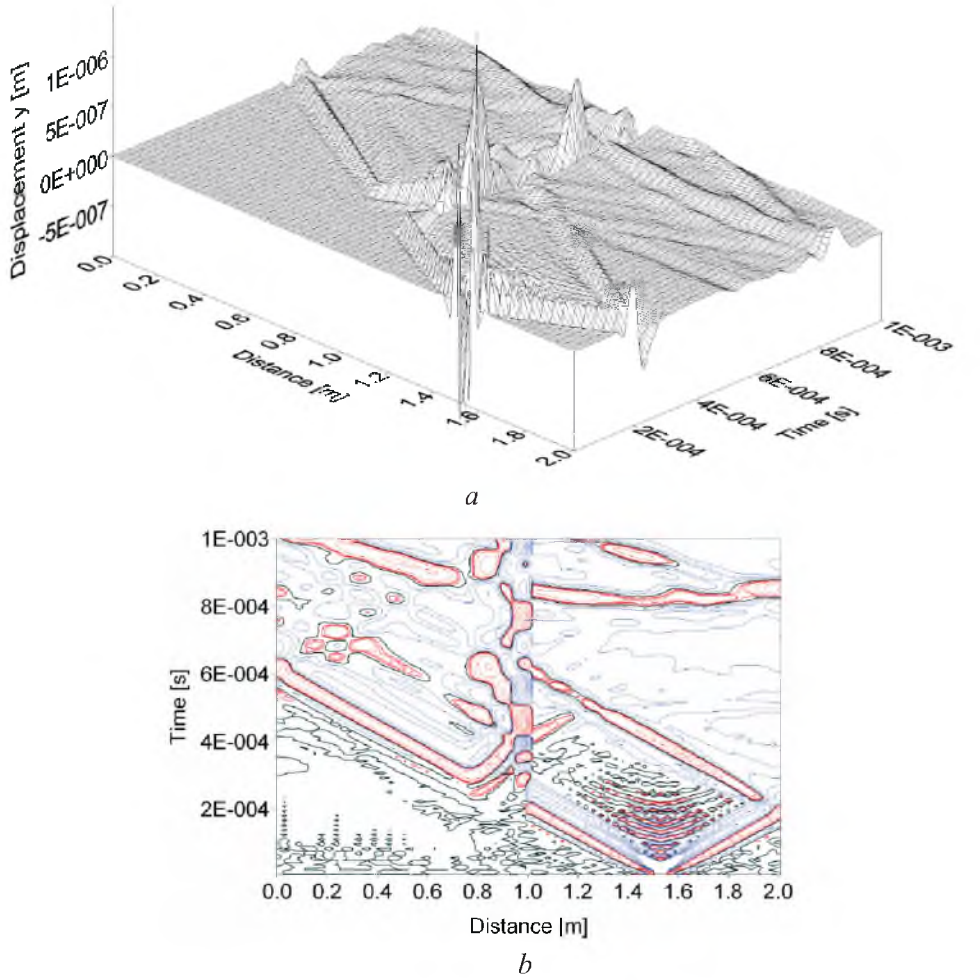

Fig. 11. Time responses from excitation in front of abuse inclined crack (170°) at the nodes along whole surface line right-angle crossing the crack (*a*) and plan view (*b*).

Surprisingly opposite tendency appears at the passing through cracks "more perpendicular" to the wall surface (approx. 45 to 135°). Waves are more damped here by acute angle (up to 90) than by obtuse angle (over 90°).

After passing through obtuse inclined cracks (over 140°) the wave "emerges" to the surface above the crack's root (being near the surface here) and propagate in both directions, i.e., partly continue farther from excitation source and from crack just overcome crack, and partly returns to the crack mouth. This wave reflects here from acute angle well and creates wave front, which propagates in a parallel way to the wave front, which passed through the crack directly. So, the passed R-wave front is split to two parts by the crack. The energy reflected from the crack's root returns back, and creates delayed reflection mentioned above (Fig. 11a and 11b). If we place the sensor unhappily above such sharply inclined crack (behind its mouth in the direction from the excitation), then the wave trajectory from excitation (and time arrival too) is artificially extended and it can results totally crack localization failure.

Generally, the differences between the time responses of waves passed through contrary inclined cracks with equal perpendicular depth (i.e., from the opposite front of crack) are greatly lesser (!) then the differences by wave reflections. Clearly it demonstrates Fig. 12, compare with Fig. 7.

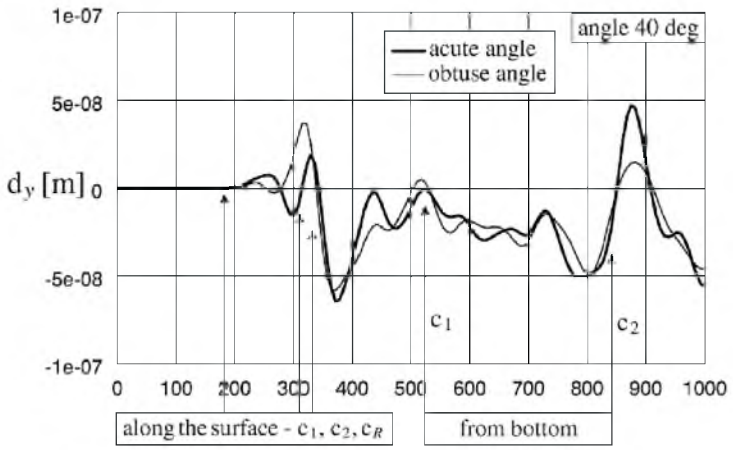

Fig. 12. The wave passing through acute crack 40° inclined and through abuse crack 140° inclined. Time dependences of displacement perpendicular to the surface.

Next will be Impact-Echo method simulation continue by walls with bulky cavities variably oriented to the surface and by simulation of enclosed crack generated by corrosion product expansion.

2.1.5. *Detection of the Internal Flat Void*. The mathematical model is similar to previous case, compare Figs. 4 and 13. The void is rectangular with dimensions 30×30 m and for example can be resulted from corrosion of reinforcing bars [3]. In the next Fig. 14 is illustrated the total deformations of the specimen at the time $t = 318$ μs when the void is just opened. As the result of individual wave fronts propagation the shape of the void is changed (opening or arresting). In the next Fig. 14 are compared two different vertical displacements of the surface. First one represents the response of specimen without void and the second one with void. In both cases the locations of the impact and sensor are identical, i.e., on the left and right edge of void, i.e., just above the void. Up to time $t = 250$ μs they are no differences in the shape of response curves. Significant are in the time interval $t \in \langle 250;\ 450 \rangle$ μs. This phenomenon may be explained as the result of reflections of the shear (c_2) and dilatation (c_1) waves from the void. Unfortunately the wave front of Rayilegh wave is dominant and thus the detection of c_1 and c_2 waves will be problematic. For the decision making if the Impact-Echo represent good tool for detection of this type of voids, the similar numerical testing shall be performed for the different depths of void.

2.2. ***Test Specimens***. The concrete specimens are illustrated in Figs. 15–18 [4]. The first one (Fig. 15) represents only testing case for calibration of measurements and for the detection of cracks with different depths (cutting is supposed). Two different reinforcing bars are used for tuning of mathematical model as presented in the Section 2.1.2.

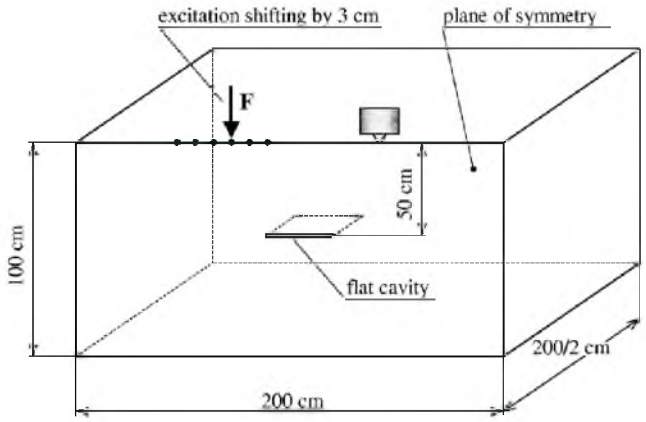

Fig. 13. Scheme of the flat crack.

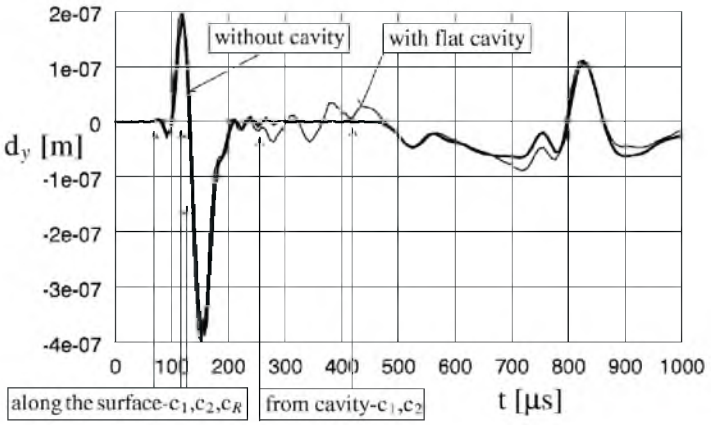

Fig. 14. Displacements of the surface in vertical direction.

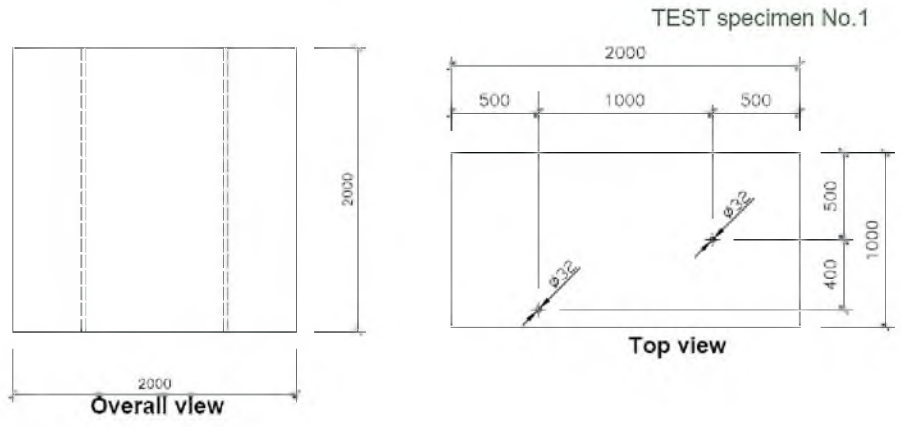

Fig. 15. Test specimen No. 1.

The second specimen (Fig. 16) will be used for the detection of imperfections in internal liners. In the longitudinal welding, there was intentionally omitted weld metal. This situation is possible in real concrete NPP structures.

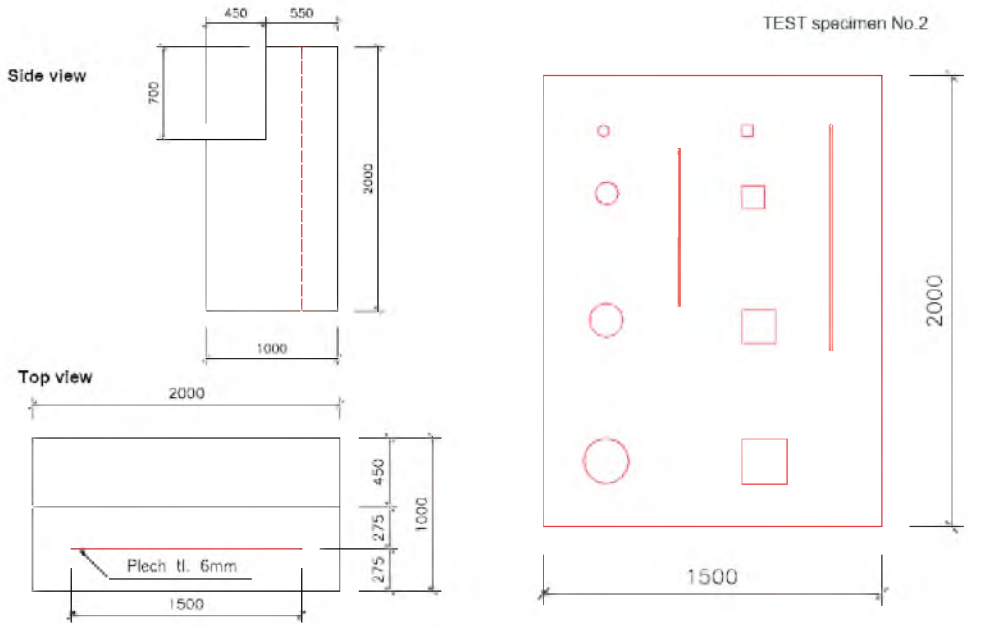

Fig. 16. Test specimen No. 2.

The third specimen (Fig. 17) is manufactured with rectangular and circular holes with different sizes. These are used for detection of tendon ducts and in combination with results of Section 2.1.5 for detection of voids in grouted tendon ducts in containment/waste store roofs. The fourth specimen (Fig. 18) represent real grid of reinforcing bars. The diameters of the bars are identical with the some ones used in NPP's with reactors VVER 440 Model 213.

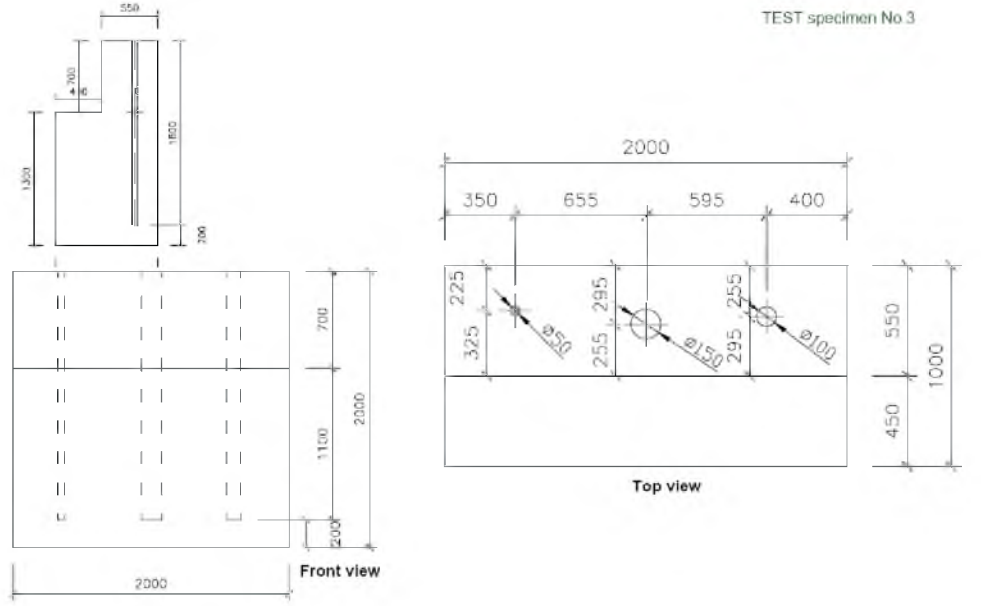

Fig. 17. Test specimen No. 3.

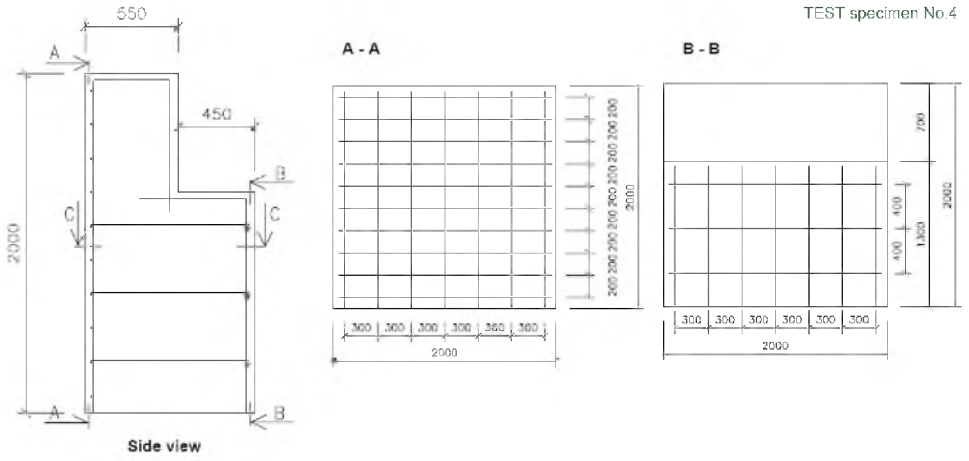

Fig. 18. Test specimen No. 4.

Conclusions. Although NDE techniques have been used successfully on a variety of reinforced and post-tensioned concrete structures, characteristics of structures in nuclear plant (section thickness, accessibility and congested reinforcement) may influence NDE results. There is a general lack of confidence in the techniques because there is little independent advice on their applicability, capability, accuracy and reliability in these circumstances. The immediate requirement is for quantification of the capabilities, base on an international standard (benchmark) application. Authoritative documentation in the form of reports and standards is desirable.

Development of NDE techniques to meet the following needs would bring high benefit:

(i) detection of corrosion in steel liners that are buried (covered by concrete) or inaccessible due to presence of moisture barriers;

(ii) detection of voids > 20 mm diameter in grouted tendon ducts in containments/waste store roofs;

(iii) improve variable performance statistics associated with depth measurement of surface cracks. For detection and sizing (depth, width, length) of cracks normal to surface aiming for sensitivity of $\pm 10\%$ for crack widths > 0.2 mm.

The most promising NDE techniques for development were identified as being radar, radiography and acoustic methods (including ultrasonic and Impact-Echo methods).

The presented NRI research and development program reflect all these items. The other non-CR institutes and NPP's are invited for participation both in measurements and theory.

Резюме

Основними проблемами ядерної енергетики є контроль за процесом старіння і відновлення операційних ліцензій існуючих атомних станцій. В якості найбільш пріоритетного направлення контролю за процесом старіння бетонних конструкцій використовуються так звані ISI-методи для залізобетонних

товстостінних конструкцій, що мають недоступні для огляду місця. Обговорюється науково-дослідна програма в цій області, а також деякі результати, що використовуються в кваліфікаційному аналізі ISI-методів.

1. L. Pecinka, S. Moravka, and J. Voldrich, "Use and performance of concrete in NPP fuel facilities," in: CSNI/RILEM Workshop Proc. (Madrid, Spain, March 2004), NEA/CSNI/R (2004).
2. S. Moravka, "Modeling of impact echo method for the detection and localization of cracks variously inclined to the surface," in: Proc. *Computational Mechanics 2005* (21th Conference with International Participation), University of West Bohemia in Pilsen (2005).
3. S. Moravka and J. Voldrich, "Mathematical modeling of variably deep surface cracks and flat voids in concrete structures using impact-echo method," in: Proc. *Computational Mechanics 2004* (20th Conference with International Participation), University of West Bohemia in Pilsen (2004).
4. J. Maly and K. Schererova, *Design of Concrete Specimens for Testing of Impact-Echo Method*, Report NRI, No. 5040-T-003305 (2005).

Received 04. 11. 2005